Quantum Monte Carlo Algorithm for Constrained Fermions: Application to the Infinite-U Hubbard Model

X. Y. Zhang, Elihu Abrahams, and G. Kotliar
Serin Physics Laboratory, Rutgers University, P.O. Box 849, Piscataway, New Jersey 08855-0849
(Received 20 November 1990)

By constructing a complete set of coherent states that forbids double occupancy, we introduce a quantum Monte Carlo algorithm for simulation of fermion models with constraint, including the infinite-U Hubbard model and the t-J model. Application to the infinite-U Hubbard model on 4×4 and 6×6 lattices provides new physical results on the thermodynamics of the model, especially the temperature and doping dependence of the Nagaoka state.

PACS numbers: 75.10.Jm

There is a class of fermion models in condensed-matter physics that has local inequality constraints, i.e., no more than one particle can occupy a given site at a given time. Among those models, the ones that have drawn most attention recently are the infinite-U Hubbard model, which we shall call the t model, and the t-J model. Numerical studies of the two models have mostly concentrated on using exact diagonalization techniques which are restricted to very small systems. To investigate systems of reasonably large size, quantum Monte Carlo simulation is useful. However, the available algorithms for simulations of the Hubbard model, although well developed and powerful, cannot incorporate the large-U limit.[1,2] Similarly, no Monte Carlo algorithm is available for the t-J model because of the constraint of no double occupancy.

We have developed a new algorithm which properly treats the constraint. We use fermion coherent states in the Hilbert space of no double occupancy ("the constrained subspace"). The constraint is enforced by an Ising-like variable defined on the spacetime lattice. After the integration of the fermion degrees of freedom, the partition function becomes a sum of determinants over the Ising variables, a natural subject for Monte Carlo simulations. We apply this algorithm to the t model and obtain some thermodynamic properties of the model which were previously unknown. In particular, we show that there is a smooth crossover from free-particle behavior at low concentration to the ferromagnetically aligned Nagaoka state near half filling. In the latter regime, we measure the magnetization and the correlation length as functions of temperature and doping and we find the effective ferromagnetic coupling.

We start with the partition function

$$Z=\mathrm{Tr}\exp[-\beta(H-\mu N)]\,, \tag{1}$$

where the trace Tr is taken in the constrained subspace. The Hamiltonian

$$H=-t\sum c_{i,\sigma}^{\dagger}c_{i+\delta,\sigma}+\mathrm{H.c.} \tag{2}$$

describes unconstrained nearest-neighbor hopping. We further decompose Z into small imaginary time steps:

$$Z=\mathrm{Tr}\prod_{1}^{L}\exp[-\Delta\tau(H-\mu N)]\,, \tag{3}$$

where $\Delta\tau L=\beta$. If at each time step a complete set of states with no double occupancy is inserted, then as $\Delta\tau\rightarrow0$ all the undesired states with double occupancy are eliminated so that Z becomes exactly the partition function for the constrained H. We choose fermion coherent states[3] to form the basis of this constrained subspace.

The state

$$|\xi\sigma\rangle=\prod_{i}(1-\xi_{i\sigma_i}c_{i\sigma_i}^{\dagger})|0\rangle\,, \tag{4}$$

where the $\xi_{i\sigma}$ are Grassmann variables and σ_i denotes either $\uparrow$ or $\downarrow$, is a fermion coherent state having a "spin configuration" $\sigma=\{\sigma_i\}$, and the property, $c_{i\uparrow}c_{i\downarrow}|\xi\sigma\rangle=0$ for any given site i. Moreover, any state that does not have double occupancy has nonzero projection to (4). Therefore $|\xi\sigma\rangle$ can be used to form a complete set for the no-double-occupancy subspace.

We construct the resolution of the identity in the subspace as follows:

$$I=\tilde{\sum}|\xi\sigma\rangle\langle\xi\sigma|\,, \tag{5}$$

where

$$\tilde{\sum}=\sum_{\sigma_1\cdots\sigma_N}\int\prod_{i}d\xi_{i\sigma_i}^{*}d\xi_{i\sigma_i}\exp\left(-\tfrac{1}{2}\sum_{i}\xi_{i\sigma_i}^{*}\xi_{i\sigma_i}\right). \tag{6}$$

One can also prove that the overlap of two coherent states from the set (4) is given by

$$\langle\xi'\sigma'|\xi''\sigma''\rangle=\langle\xi'\sigma'|I|\xi''\sigma''\rangle=\exp\sum_{i}\delta_{\sigma_i'\sigma_i''}\xi_{i\sigma_i'}'^{*}\xi_{i\sigma_i''}''\,. \tag{7}$$

The weight function in Eq. (6) differs from the norm $\langle\xi\sigma|\xi\sigma\rangle$ by the factor $\frac{1}{2}$ in the exponent. This compensates the overcounting of states (in addition to the known overcompleteness of the coherent states) when Eq. (4) is used as basis. The trace operator Tr is constructed similarly:

$$\mathrm{Tr}A=\tilde{\sum}\langle-\xi\sigma|A|\xi\sigma\rangle\,. \tag{8}$$

We now insert the identity operator defined above at each time slice in Eq. (3) and take the trace using Eq. (8). The partition function becomes

$$Z=\sum_{\{\sigma_i^l\}}\int\prod_{l,i}d\xi_{i\sigma_i^l}^{l*}d\xi_{i\sigma_i^l}^{l}\exp\left(-\tfrac{1}{2}\sum_i\xi_{i\sigma_i^l}^{l*}\xi_{i\sigma_i^l}^{l}\right)\langle\xi^l\sigma^l|\xi^{l-1}\sigma^{l-1}\rangle\exp[-\Delta\tau\langle\xi^l\sigma^l|H-\mu N|\xi^{l-1}\sigma^{l-1}\rangle]\,. \tag{9}$$

The overlap $\langle\xi^l\sigma^l|\xi^{l-1}\sigma^{l-1}\rangle$ is obtained from Eq. (7). Although H defined in Eq. (2) has two independent hopping terms, one for spin up and one for spin down, the no-double-occupancy coherent states inserted at each time slice have only one spin at a site. Therefore,

$$\langle\xi^l\sigma^l|H|\xi^{l-1}\sigma^{l-1}\rangle=-t\sum_{ij}\xi_{i\sigma_i^l}^{l*}\xi_{j\sigma_j^{l-1}}^{l-1}\delta_{\sigma_i^l\sigma_j^{l-1}} \tag{10}$$

has one hopping term only. The appearance of the δ function reflects the fact that hopping conserves spin. This result for the partition function shows how the constraint of no double occupancy is effectively accounted for by attaching a spin variable to each site, rather than to the particles.

The integrand of the partition function has the form $\exp(\sum\xi_a^*M_{ab}\xi_b)$, where a denotes the set (i,σ,l) of sites, spins, and time slices. The integration over the Grassmann variables then leads, as usual, to $\det M$. Explicitly,

$$Z=\sum_{\{\sigma_i^l=\uparrow,\downarrow\}}\det(2^{-L}I+B_1\cdots B_L)\,, \tag{11}$$

where

$$(B_l)_{ij}=\delta_{\sigma_i^l\sigma_j^{l-1}}B_{ij}^0 \tag{12}$$

and B_{ij}^0 is the single-particle hopping matrix

$$B_{ij}^0=\delta_{ij}-\Delta\tau(H_{ij}-\mu\delta_{ij})\approx\exp[-\Delta\tau(H_{ij}-\mu\delta_{ij})]\,, \tag{13}$$

where $H_{ij}=-t$ for nearest neighbors and zero otherwise.

To derive a few known results, we first notice that the nth-order term in the expansion of the determinant

$$\det(I+M)=1+\mathrm{Tr}M+\cdots+\det(M) \tag{14}$$

represents an n-particle partition function. We can expand Eq. (11) accordingly. For the zero-particle case, we have $Z_0=\sum 2^{-LN}=1$. We see that the factor $\frac{1}{2}$ compensates the overcounting of the vacuum state.

Next, we obtain Z_1 from Eqs. (11) and (14) as

$$Z_1=2^{-NL}\sum_{\{\sigma_i^l\}}\mathrm{Tr}[2^LB_1\cdots B_L]\,. \tag{15}$$

All the spin sums from the various time slices are evaluated via the δ functions. The result is

$$Z_1=2\,\mathrm{Tr}B^L=2\sum_k\exp[-\beta(\varepsilon_k-\mu)]\,, \tag{16}$$

which is the expected doubly degenerate single-particle partition function.

The N-particle case is the "half-filled" t model. We have

$$Z_N=\sum_{\{\sigma_i^l\}}\det(B_1\cdots B_L)=\sum\prod_l\det(B_l)\,. \tag{17}$$

We can successively sum the spin configurations of the intermediate time slices. The final sum is for the Lth slice

$$\sum_{\{\sigma^L\}}\det(B^L)_{LL}=2^N\det(B^0)^L=2^N\,. \tag{18}$$

So the partition function for the half-filled case is fully degenerate, as is known.

Equation (11) provides a natural algorithm for quantum Monte Carlo simulations. Formally, it resembles the discrete Hubbard-Stratonovich transformation introduced by Hirsch[4] for the Hubbard model, with the σ_i^l playing the role of auxiliary fields. As in that case, the σ's are related to the z component of the magnetization although in a slightly different way which will be shown below. Since the entire derivation is independent of the details of the B matrix, one can add other hopping terms to the Hamiltonian, for example, the diagonal hopping t'. One can also add a Heisenberg interaction by representing the spins in terms of the Grassmann variables and the interaction in terms of a sum over a discrete Hubbard-Stratonovich field s_{ij} as

$$\langle\xi_\sigma^{l+1}|\exp[-\Delta\tau JS_i^+S_j^-]|\xi_\sigma^l\rangle=\tfrac{1}{2}\langle\xi_\sigma^{l+1}|\xi_\sigma^l\rangle\delta_{\sigma^{l+1}\sigma^l}\sum_{s_{ij}}\exp[\sqrt{\Delta\tau J/2}\,s_{ij}(\xi_{i\sigma}^{*l+1}\xi_{j\sigma}^l+\xi_{j\sigma}^{*l+1}\xi_{i\sigma}^l)]\,. \tag{19}$$

The interaction along the z component is decoupled similarly. Now the problem reduces to the original t model with hopping matrix elements which depend on space and time through s_{ij}. Thus the algorithm can be used to simulate a variety of models, including the t-t'-J model.

We now briefly discuss our Monte Carlo updating and measurement scheme and present some results for the t model.

It is clear from (12) that a local spin flip at time slice l and site i results in a nonlocal change of the matrix elements in the ith row of B_l and the ith column of B_{l+1}. The method developed by Blankenbecler, Scalapino, and Sugar[5] can be applied only after certain modifications.[6] To ease the initial implementation of our method, we have used a straightforward updating routine by reevaluating the determinant after each change of configuration. The computing time scales as LN^4. At lower temperatures, the stabilized Green's-function updating methods discussed in Refs. 1 and 2 would most likely be necessary instead of our determinantal updating procedure.

We measure three quantities, the magnetization, the particle number, and the total energy of the system. They are all determined by the equal-time Green's function $g(i,j)$, as in other quantum Monte Carlo simula-

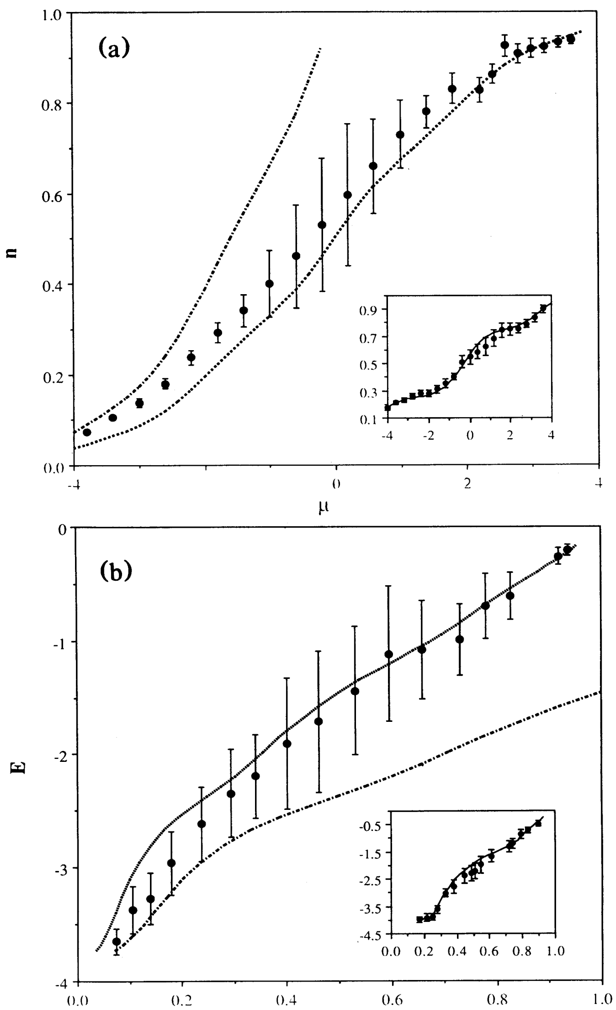

FIG. 1. 4×4 lattice. (a) The particle density vs the chemical potential. The top dotted line is for free particle and the bottom dotted line is for Nagaoka state. Inset: Comparison to the exact result on the 2×2 lattice. (b) The energy per particle vs concentration. The top dotted line is for Nagaoka state and the bottom one is for the free particle. Inset: Comparison to the exact result on the 2×2 lattice.

tions:

$$g(i,j) = Z^{-1}\mathrm{Tr}\, e^{-\beta H}(c_{i\uparrow}c_{j\uparrow}^{\dagger} + c_{i\downarrow}c_{j\downarrow}^{\dagger}) = Z^{-1}\sum_{\sigma} M_{ij}^{-1}(\sigma)\,, \tag{20}$$

where

$$M_{ij}^{-1} = 2^{-L+1}[(2^{-L}I + B_1 \cdots B_L)^{-1}]_{ij}\,. \tag{21}$$

The total energy of the system is the hopping energy

$$E = \left\langle -t\sum_{ij\sigma} c_{i\sigma}^{\dagger}c_{j\sigma}\right\rangle = t\sum_{ij} g(i,j)\,. \tag{22}$$

The average particle number is $\langle n_i \rangle = 1 - g(i,i)/2$, where the operator identity $n_i = 1 - (c_{i\uparrow}c_{i\uparrow}^{\dagger} + c_{i\downarrow}c_{i\downarrow}^{\dagger})/2$ has been used in the subspace of no double occupancy. One can prove that the average magnetization is given by

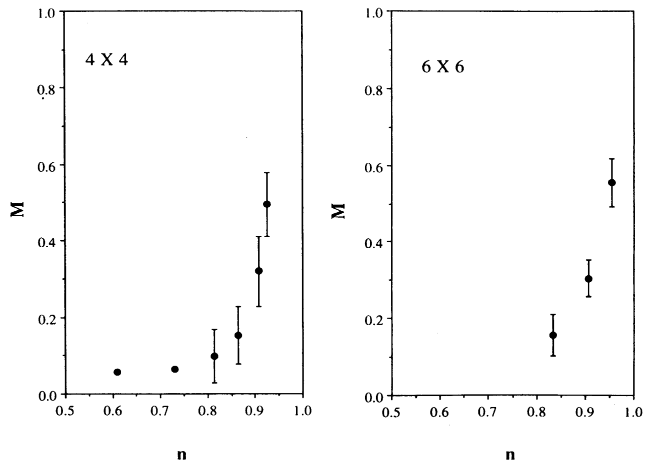

FIG. 2. Average magnetization per particle vs the particle concentration. The error bars for the particle concentration are small: 4×4 lattice and 6×6.

$\langle m_{iz} \rangle = \langle n_{i\sigma_i}\sigma_i \rangle$.

We performed simulations on 2×2, 4×4, and 6×6 lattices with temperatures mostly at $\beta = 2$. The energy scale is normalized to t. We chose $\Delta\tau$ to be 0.1 so that $L = 20$. The error due to finite $\Delta\tau$ in projecting out the sub-Hilbert space is estimated to be proportional to $\Delta\tau$.[7] There are negative weights which occur most frequently at and above about quarter filling for the range of temperature we simulated.[8] In the regime of density close to half filling ($0.9 < \langle n \rangle \le 1$), where there is a ferromagnetic order, there are many metastable states that make the final results sensitive to the initial condition. We added some global moves in the updating routine and we averaged over various initial conditions to avoid the possibility of biased sampling.

To check the updating scheme, we made a comparison to the exact diagonalization result on the 2×2 lattice and found good agreement, as shown in the inset in Figs. 1(a) and 1(b). Figures 1(a) and 1(b) are the data obtained from the 4×4 lattice, which show a crossover from free-particle behavior at low concentration to the ferromagnetic Nagaoka state at high concentration. The data obtained from the 6×6 lattice exhibit similar behavior. A number of studies have addressed the issue of the ground-state property of the t model: I.e., how far from half filling does the Nagaoka state remain stable?[9,10] In order to study the Nagaoka state at finite temperature, we applied a very small magnetic field in the z direction. Various field strengths ranging from $0.01t$ to $0.1t$ are used to extrapolate the zero-field information. As shown in Fig. 2, the magnetization decays exponentially with doping. However, the energy of the Nagaoka state remains competitive in a rather large doping range as shown in Fig. 1. Although the simulation was performed on a finite-size lattice, we found no significant irregular behavior such as magnetization oscillations as a function of doping.[10] This is due to the

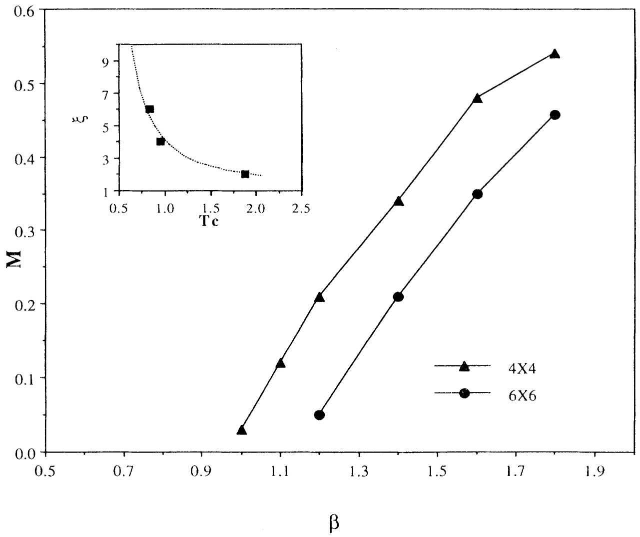

FIG. 3. Average magnetization per particle vs inverse temperature on 6×6 and 4×4 lattices. Error bars are neglected. The interesting points where the two curves intersect the β axis have little fluctuation. Inset: Temperature dependence of the ferromagnetic correlation length. The analytic result for the 2×2 lattice is included.

effect of finite temperature and the fact that the particle number was not fixed in the simulation.

Since the Nagaoka state processes a SU(2) symmetry, the average magnetization should be zero at finite temperature in two dimensions. The reason that we have observed a nonzero M_z is due to a finite-size effect; i.e., the correlation length ξ becomes greater than the sample size below a certain temperature. We make use of this effect and determine the temperature dependence of the correlation length by measuring the magnetization as a function of temperature for a given concentration. The results are shown in Fig. 3 for the 6×6 and 4×4 lattices. The inset in Fig. 3 shows the resulting temperature dependence of ξ. It fits well with the expected universal form $\xi \propto \exp(4\pi\mathcal{J}/T)$ calculated from a renormalization-group analysis,[11] with an effective coupling $\mathcal{J} \approx 0.1t$. Figure 3 demonstrates to a certain degree the reliability of the simulation because the $\xi = 2$ point is calculated analytically.

To conclude, we have developed a new fermion quantum Monte Carlo algorithm specifically designed for handling the no-double-occupancy constraint, which can be used for simulations of the t model, the t-J model, and other related fermion models. We demonstrated the usefulness of the algorithm through simulations of the t model and, in the process, provided some new results on the thermodynamics of the infinite-U Hubbard model.

One of us (X.Y.Z.) is grateful to A. Ruckenstein and N. Andrei for encouragement. We thank E. Brézin, P. Coleman, J. C. Angles-D'Auriac, G. S. Grest, T. Kopp, R. Sugar, D. J. Scalapino, R. M. Fye, and R. T. Scalettar for many useful discussions. This work was partially supported by the National Science Foundation under Grants No. DMR 89-06958 and No. DMR 89-96285. We utilized the Cray X-MP/48 system at the National Center for Supercomputing Applications, University of Illinois at Urbana-Champaign.

[1]D. J. Scalapino, R. L. Sugar, S. R. White, N. E. Bickers, and R. T. Scalettar, Phys. Scr. **T27**, 101 (1989).

[2]For a detailed review, see E. Y. Loh, Jr., and J. E. Gubernatis, in *Electronic Phase Transitions,* edited by W. Hanke and Y. V. Kopaev (Elsevier, New York, 1990).

[3]See, for example, J. Negele and H. Orland, *Quantum Many-Particle Systems* (Addison-Wesley, London, 1988).

[4]J. E. Hirsch, Phys. Rev. B **28**, 4059 (1983).

[5]R. Blankenbecler, D. J. Scalapino, and R. L. Sugar, Phys. Rev. D **24**, 2278 (1981).

[6]R. L. Sugar (private communication).

[7]R. M. Fye (unpublished).

[8]For example, the worst case for the 4×4 lattice at $\beta = 2$ occurs just above quarter filling, where the average sign is 0.45.

[9]B. S. Shastry, H. R. Krishnamurthy, and P. W. Anderson, Phys. Rev. B **41**, 2375 (1990).

[10]Y. Fang, A. E. Ruckenstein, E. Dagoto, and S. Schmitt-Rink, Phys. Rev. B **40**, 7406 (1989); J. A. Riera and A. P. Young, Phys. Rev. B **40**, 5285 (1989).

[11]A. M. Polyakov, Phys. Lett. **59B**, 79 (1975).